

STM microcontroller implementation of MPPT algorithms for stand-alone PV Water Pumping System

Rabiah Gammoudi, Najet Rebei, Othman Hasnaoui

Abstract— Recently, the attention has focused on the optimal operation of the PVG to obtain the most reliable and economic operation order the nonlinearity of PV Generator and the high dependence on weather conditions.

In this work, we will validate in real time and compare two MPPT approaches. The proposed approaches in this paper are the constant voltage approach (CV) and Incremental Conductance approach (IC) with sudden and random variations of insolation applied to a photovoltaic water pumping system (PVWPS) in order to optimize the photovoltaic power generation and extract the maximum power. The PVWPS includes a PV Generator, a boost converter, an inverter type SEMIKRON and a centrifugal pump LOWARA (CEA70/3/A). The control part is provided by STM32F4 microcontroller running environment Matlab/Simulink, and we use a computer incorporating a card DS1104 for acquisition. Also, a comparative study is made between these two types of methods. The results obtained show the usefulness of the developed algorithms in solving the problem of degradation of PVG performance depending on the variation of climatic factors with a very good efficiency.

Index Terms—PV Generator (PVG), Maximum Power Point Tracking (MPPT), PV Water Pumping System (PVWPS), Constant Voltage method (CV), Incremental Conductance method (IC).

I. INTRODUCTION

Nowadays, the consumption of electrical energy is increasingly growing in the world. This increase affects both developing countries, industrialized countries and causes environmental problems. We live in times of a great need for research a new power generation solutions; cleaner and more sustainable sources than standard energy power plants using oil, gas and uranium. The solutions adopted are essentially based on renewable energy such as wind, geothermal or photovoltaic energy. Today, renewable energy has become an absolute necessity view the very expensive oil prices and the resulting pollution by the wide use of these energies, [1]. The development renewable energy is essential to ensure energy independence and meet the climate challenge. Photovoltaic is one of these energies that are an environmentally friendly source of electricity. Despite the considerable distance between the sun and the earth (150,106 Km), terrestrial layer receives a significant amount of energy 180 106 GW that can meet the energy needs of the globe, [2]. The Systems applications of photovoltaic production may be independent (water pumping, electric vehicles, public lighting) or connected to the grid (power plants). The photovoltaic pumping is one of the promising applications of the use of photovoltaic energy especially in sub-Saharan countries where their power networks still don't manage to cover all

residents. However the operation of the PV power has certain problems; the high cost, the low yield (8% -17%) of the PV array and the dependence on climatic factors require an optimal and rational use of the latter to reach an economical and profitable operation, [3]. In this context, scientific research is aimed at developing effective optimization methods for determining the maximum power point "MPP" of the P-V characteristic for a PVG to different climatic conditions. In the scientific literature, several techniques of MPPT control are proposed and developed by researchers. These MPPT methods are classified into two categories indirect and direct methods. The indirect methods use databases of PV characteristics in different climate conditions, as the open circuit method, the constant voltage method, the short circuit method, the curve-fitting method, the look-up table method. The direct methods are based on dynamic algorithm. We find different methods as perturb and observe incremental conductance, [4, 5].

This work is the introduction of a test bench for extracting maximum power from a water pumping system with a random scenario of illumination. This PVWPS is powered by a photovoltaic generator consisting of ten panels in series.

In this paper, the first part is focused on the components modeling of the PV water pumping system. The second part presented the MPPT approaches study. We are interested hereto the constant voltage and the incremental conductance methods. Finally, we implement the approaches on microcontroller STM32F4 and we ended with a comparative study between the two approaches.

II. MODELING OF THE PV WATER PUMPING SYSTEM

The experimental photovoltaic pumping system consists of a PV Generator, a boost converter, a DC-AC inverter, a STM32F4 microcontroller, a dSpace DS1104 card, a moto-pump and some sensors. Fig.1 gives the components of the experimental test bench used in this application. We note here that the Dspace DS1104 card is used for acquisition of the input and output quantities.

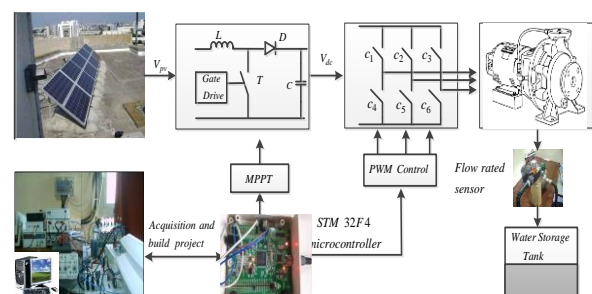


Fig.1. The experimental system bloc diagram

A. PV Generator

The PVG is constituted by an assembly of photovoltaic panels; the panels in turn are constituted by photovoltaic cells. The output quantities (voltage and current) depend on the climatic condition. The electrical specifications of the solar module used are given in appendix (1).

Modelling of solar cell

The equivalent circuit of real photovoltaic cell used as presented in the Fig.2.

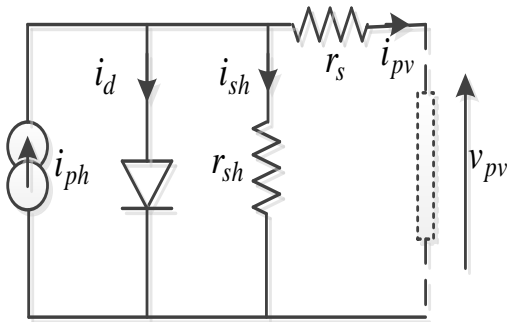


FIG.2. EQUIVALENT CIRCUIT OF REAL SOLAR CELL

The PVG mathematic model with n_s series connected solar cells, N_s series connected panels and N_p parallel connected panels are given by equation (1) with; V_{pv} and I_{pv} are respectively the output voltage and the output current of PV Generator, i_{ph} is the photocurrent, i_s is the reverse saturation current of the diode, v_t is the solar cell thermal voltage, R_s and R_{sh} are respectively the series and shunt resistors of the PVG, [6].

$$f(V_{pv}, I_{pv}) = N_p \times i_p + N_p \times i_s \left(\exp\left(\frac{n_s \times N_s \times v_{pv} + R_s \times N_p \times i_{pv}}{n_s \times N_s \times v_t}\right) - 1 \right) + \frac{n_s \times N_s \times v_{pv} + R_s \times N_p \times i_{pv}}{R_{sh}} \quad (1)$$

Experimental characteristics: Influence of climatic conditions

An experimental data base has been realized on PVG for different insolation and different temperature. We obtained then characteristics $P = f(V_{pv})$ and $I_{pv} = f(V_{pv})$ of one panel. From these characteristics, we can determine the maximum power point (MPP) that provides an optimal operation. This point is characterized by an optimum voltage V_{pvopt} and an optimum current I_{pvopt} . These quantities offer an optimum power that we want to extract. This MPP is highly dependent on weather conditions. Fig.3 and Fig.4 show the power-voltage and current-voltage characteristics of one panel.

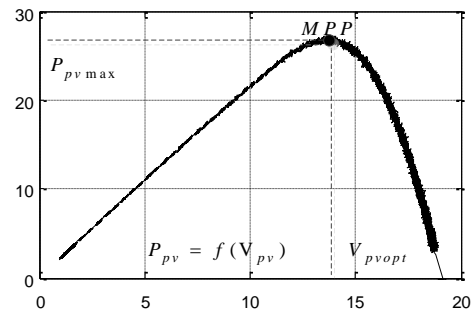


FIG.3. $P = f(V_{pv})$ CHARACTERISTIC

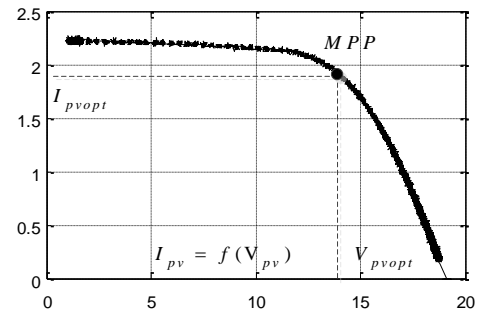


FIG.4. $I_{pv} = f(V_{pv})$ CHARACTERISTIC

To show the influence of the insolation, we have used the database. The curves in Fig.5 and Fig.6 represent the evolution of real variables voltage and power for a temperature equal to 26°C and an insolation worth 200, 300, 400, 600 and 900 Wc / m².

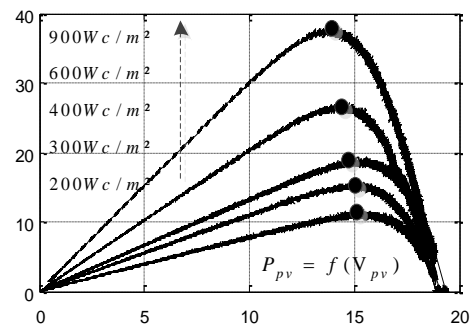


FIG.5. $P = f(V_{pv})$ CHARACTERISTIC

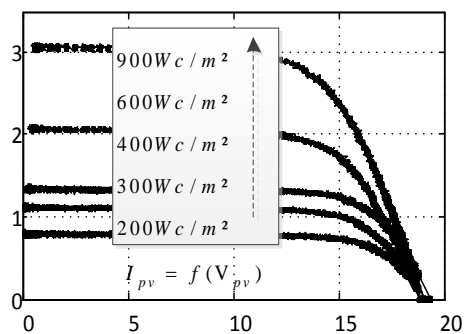


FIG.6. $I_{pv} = f(V_{pv})$ CHARACTERISTIC

We note that the short circuit current varies in the same behavior with insolation but the open circuit voltage V_{oc} doesn't vary. The maximum power is sensitive to

insolation. From $P = f(V_{pv})$ and $I_{pv} = f(V_{pv})$ characteristics, the relationship have been identified by equation (2) where the constant K_{cc} is equal to 0.89.

$$I_{pv_opt} = K_{cc} \times I_{cc} \quad (2)$$

To show the temperature influence, the insolation value is fixed at 600W/m^2 . These curves $P = f(V_{pv})$ and $I_{pv} = f(V_{pv})$ in Fig.7 and Fig.8 correspond to the variation of temperature between 23°C and 29°C .

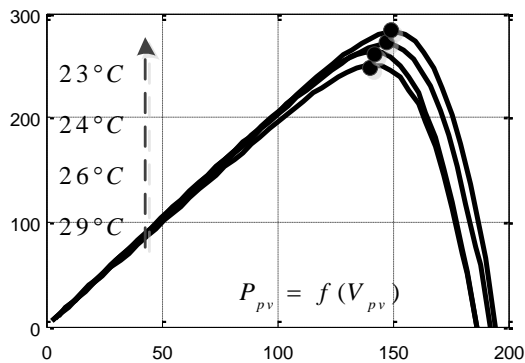


FIG.7. $P = f(V_{pv})$ CHARACTERISTIC

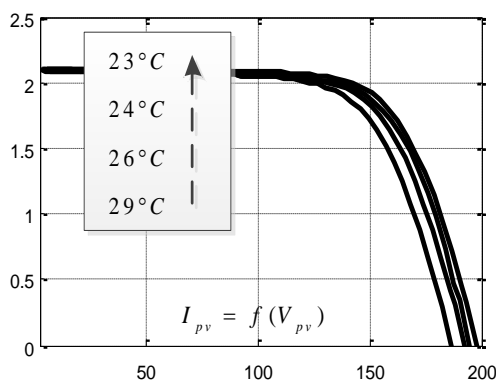


FIG.8. $I_{pv} = f(V_{pv})$ CHARACTERISTIC

The open circuit voltage is greatly influenced by the temperature change; it varies in the opposite sense, it's the same for the maximum power. Or the short circuit current is independent of temperature. From Fig.7, and Fig.8, the equation (3) gives the relation between V_{co} and V_{opt} where the constant K_{oc} is equal to 0.77.

$$V_{pv_opt} = K_{oc} \times V_{oc} \quad (3)$$

B. Boost chopper

For this chopper configuration, his average output voltage is greater than the input value, hence its name booster. This structure requires a controlled switch and a diode. Fig.6 shows the block diagram of a boost chopper: It consists of the power switch T, boost inductor L, filter capacitor C, output diode D and load resistor R. Here, the DC input source voltage is supplied by the PVG, [7].

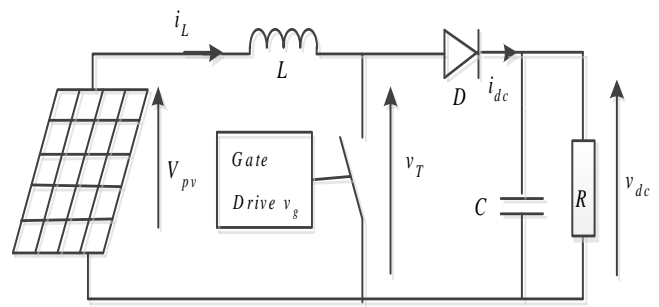


FIG.9.BOOST COPPER BLOCK DIAGRAM

When the switch T is in the on state, the current in the boost inductor increases linearly, and at that time, the diode is in the off state. When the switch T is turned off, the energy stored in the inductor is released through the diode to the output RC load. The current oscillation is smoothed by the inductance and a DC voltage oscillation is reduced by the capacitor. The boost converter transfer function is obtained by considering its steady state operation [8]. If f is the switching frequency, α is the duty ratio and R is the load resistance, the DC voltage transfer function is:

$$V_{dc} = \frac{V_{pv}}{1 - \alpha} \quad (4)$$

The boost converter operates in the continuous conduction for $L > L_{min}$ where:

$$L_{min} = \frac{(1 - \alpha)^2 \alpha R}{2f} \quad (5)$$

The minimum capacitor value that results in voltage ripple ΔV_{dc} is given by:

$$C_{min} = \frac{\alpha V_{dc}}{\Delta V_{dc} R f} \quad (6)$$

The DC-DC converter is needed for two reasons: implement the MPPT algorithm and bring the DC voltage to an acceptable level to power the load.

C. DC/AC inverter

The inverter is SEMIKRON type. Its output voltage \bar{v}_s applied to the motor is only dependent on the DC voltage (V_{dc}) and the logic states of the switches c_1 , c_2 and c_3 . Since, the studied system is assumed balanced. The associated space voltage vector in the fixed reference frame, named also Concordia's axis, is given by the equation (7).

$$\bar{v}_s = v_d + jv_q = \sqrt{\frac{2}{3}} V_{dc} [c_1 + \bar{a} c_2 + \bar{a}^2 c_3], \quad (7)$$

$$\bar{a} = e^{j\frac{2\pi}{3}}$$

The SPWM technique exploits the space vector voltage diagram and synthesizes the reference voltage vector applied \bar{v}_{sref} from the 2 neighboring vectors \bar{v}_{sk} , $\bar{v}_{s(k+1)}$ and

the zero vectors. The vectors \bar{v}_{sk} and $\bar{v}_{s(k+1)}$ are respectively applied during time intervals τ_k, τ_{k+1} and the zero vector is applied in the remaining time $\tau_0 = T_s - \tau_k - \tau_{k+1}$. Fig.10 shows the synthesis technique of SPWM.

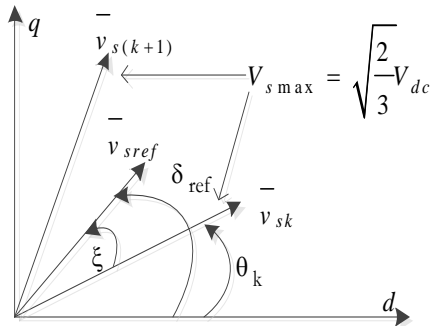


FIG.10.SYNTHESIS TECHNIQUE OF SPWM

To obtain an average value of \bar{v}_{sref} on the period T_s , there must be:

$$\frac{\tau_k \cdot \bar{v}_{sk} + \tau_{k+1} \cdot \bar{v}_{s(k+1)}}{T_s} = \bar{v}_{sref} \quad (8)$$

To comply with the constraint $\tau_k + \tau_{k+1} \leq T_s$, the module V_{sref} of the voltage vector \bar{v}_{sref} must check the condition: $V_{sref} \leq \frac{V_{dc}}{\sqrt{2}}$. In this context, the synthesis solution is as follows; the coefficient ρ is the duty cycle.

$$\tau_k = T_s \rho \sin\left(\frac{\pi}{3} - \xi\right) \quad \tau_{k+1} = T_s \rho \sin(\xi) \quad \rho = \frac{\sqrt{2} V_{sref}}{V_{dc}} \quad (9)$$

D. Moto-Pump

The pump that is used in this work is a centrifugal pump type LOWARA SM63 BG/304; the power is equal to 0.61KW. This pump is equipped with a flow rate sensor. The centrifugal pump is also described by an H (Q) characteristic given by:

$$H = A_1 \omega_r^2 - A_2 \omega_r Q - A_3 Q^2 \quad (10)$$

Where: $A_1 = 0.039$, $A_2 = -0.3079$, $A_3 = -0.0024$.

All machine parameters are given in appendix 2.

E. STM32F4 microcontroller

The STM32F4 microcontroller is designed for real-time applications. It is characterized by an optimized structure for the large amount treatment of instruction in parallel on each clock cycle. It belongs to the family ARM Cortex-M4 32-bit and controlled by an external clock signal with frequency 168MHz. Its main features are:

- 192 KB of RAM and 1 Mbyte of flash memory, which allows the implementation of complex algorithms,
- Ultra-Low dynamic power, $RTC < 1\mu A$,

- Up To 71 port inputs and outputs with a switching frequency that can reach up to 84MHz,
- It May issue a PWM signals with frequency 168MHz,
- 3 analogue converters with a resolution 12 bit and a sampling rate of 0.41μs,
- 6 USART operate at a speed of 10.5Mbyte/s.

III. MPPT APPROACHES

Two MPPT approaches are developed. The first called "Constant Voltage (CV)" method and the second is "Incremental Conductance (IC)" method.

A. Constant Voltage method

From the database, the optimum voltage is in the range of 150V with a relative error of 4%. The PVG consists to the association of 10 solar panels in series. So, to extract the maximum power it is necessary that the PV system operate at this voltage. This value will be used as reference voltage value V_{pv_ref} . This method is called "Constant Voltage (CV)". The CV approach needs the measurement of the PV array voltage in order to setup the duty-cycle of the DC/DC converter, [9, 10, 11].

B. Incremental Conductance method

Incremental conductance algorithm is based on the following equation

$$\frac{dI_{pv}}{dV_{pv}} + \frac{I_{pv}}{V_{pv}} = 0 \quad (11)$$

When the operating point is in the right of the maximum power point, so we have:

$$\frac{dI_{pv}}{dV_{pv}} + \frac{I_{pv}}{V_{pv}} < 0 \quad (12)$$

If this point is to left of maximum power point, we obtained:

$$\frac{dI_{pv}}{dV_{pv}} + \frac{I_{pv}}{V_{pv}} > 0 \quad (13)$$

The optimum can be followed by comparing the instantaneous conductance $\frac{I_{pv}}{V_{pv}}$ and the incremental

conductance $\frac{dI_{pv}}{dV_{pv}}$. If the optimum is reached, the operation

of the PVG is maintained at this point and the disturbance stops until a new change in current level is noted, [12, 13, 14]. In this case, the decrease in the algorithm or the increment is performed to follow the new maximum power point; the size of the increment determines the speed to follow the maximum power point. This method provides a good performance in rapidly changing weather conditions. Fig.11 shows that from an operating point A, if weather conditions are invariable, a disturbance ΔV_{pv} brings the operating point B and the disturbance will be canceled due to a decrease in power. All times the illumination increases and moves the power curve from P1 to P2, the operating point also moves from A to C.

This displacement represents an increase in power and the perturbation is kept the same.

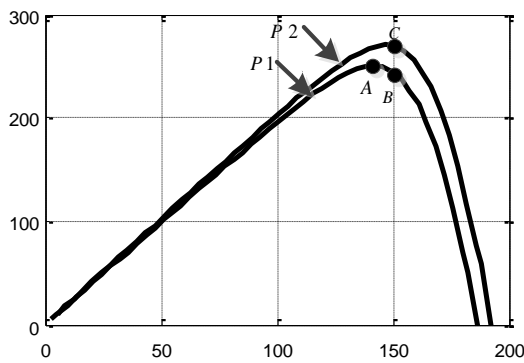


FIG.11.DIVERGENCE OF IC FROM MPP

C. Estimation of maximum power

The estimated optimal power is defined by the equation (14). This optimal power depends strongly on weather conditions. This is shown by the following equations:

$$P_{pv-opt} = V_{pv-opt} \cdot I_{pv-opt} \quad (14)$$

The efficiency is the ratio of the actual PVG extracted power and the estimated maximum power.

$$h = \frac{P_{pv-opt}}{P_{pv}} \quad (15)$$

IV. EXPERIMENTAL RESULTS

The knowledge of quantities current and voltage is crucial. These quantities are measured respectively by a current sensor LA25 NP and a voltage sensor LV25-P. The temperature sensor used for this application is based on LM335. The insolation sensor use the short current principle.

Two approaches are implemented on STM32f4 to examine the two control algorithms. One is for the constant voltage criterion the other for the incremental conductance. We note here that every approach has an appropriate insolation scenario.

A. CV results

The CV approach implemented on STM32F4 microcontroller is given by Fig.9. The project is build. In the first step, we start with the acquisition of the PVG voltage V_{pv} and stator voltage V_s through sensors voltage with a proportionality factor equal to 87.72. The stator voltage V_s is divided by the nominal flux to determine the pulsation. The blocks Reference_source1, SYM_SPWM and Basic PWM1 give the commands c_1 , c_2 and c_3 of switches. Then, we compare PVG voltage V_{pv} to a reference voltage. The output feed the chopper.

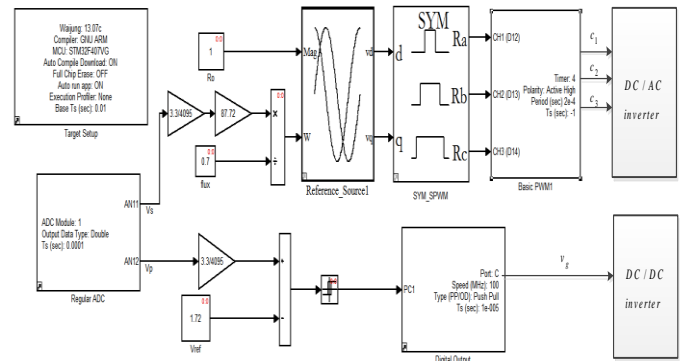


FIG.12.THE CV APPROACH IMPLEMENTED ON STM32F4

We reconstitute from the outputs C_1 , C_2 and C_3 , the stator voltage components V_d and V_q as presented respectively in Fig.13 and Fig.14.

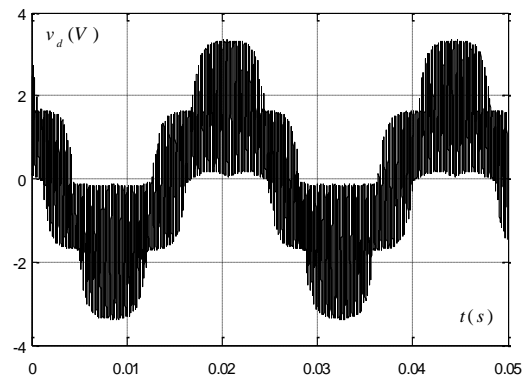


FIG.13.DIRECT COMPONENT VOLTAGE

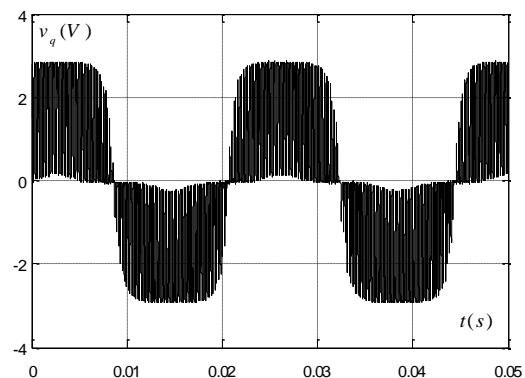


FIG.14.QUADRATURE COMPONENT VOLTAGE

The following figures show the experimental results for a temperature equal to 26° and under insolation variation. For a real scenario presented by Fig.15, the insolation changes between 300 and 900Wc / m². Fig.16 gives the evolution of the extracted power P_{pv} , the estimated maximum power P_{pv-opt} and the efficiency that can research 96%.

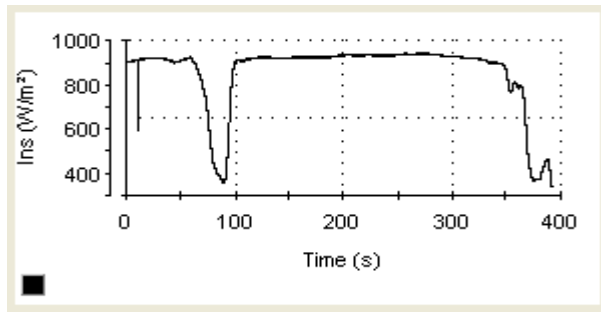


FIG.15. EVOLUTION OF INSOLATION

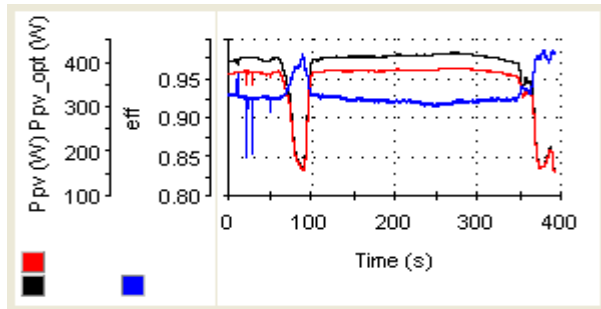


FIG.16. EXTRACTED, OPTIMAL AND EFFICIENCY

Fig.17 illustrates respectively the voltages V_{pv} , V_{dc} and V_{pv_opt} . The PVG voltage V_{pv} carried his reference. The operating point displacement for the proposed scenario is given in Fig.18, the maximum power point is always close to the reference voltage corresponding to an optimal operating which confirming the validity of the approach.

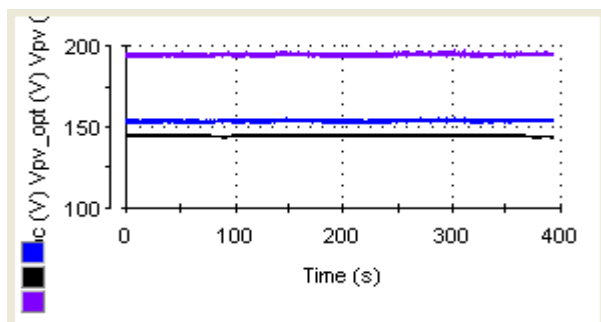
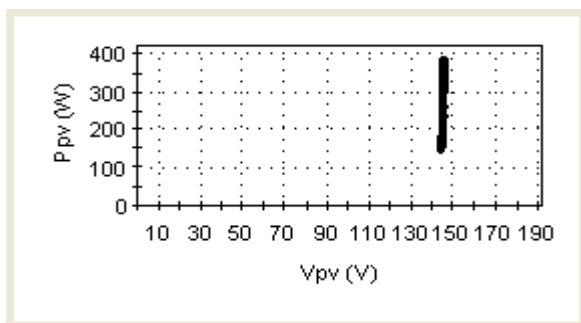

 FIG.17. EVOLUTION OF V_{dc} , V_{pv} AND V_{pv_opt}


FIG.18. MPP EVOLUTION

The effect of the operation at maximum power point on the pump is mentioned in Fig.19 and Fig.20. The stator pulsation vary together to have a constant flux. The flow rate and the electromagnetic torque have the similar evolution as insolation. The flow rate is evolved with the insolation and its maximum value is obtained if the maximum power point is determined effectively.

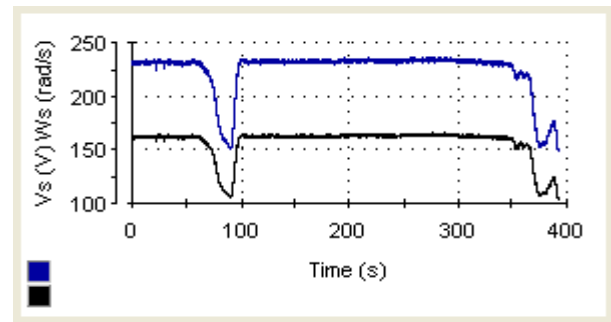


FIG.19. EVOLUTION OF STATOR VOLTAGE AND PULSATION

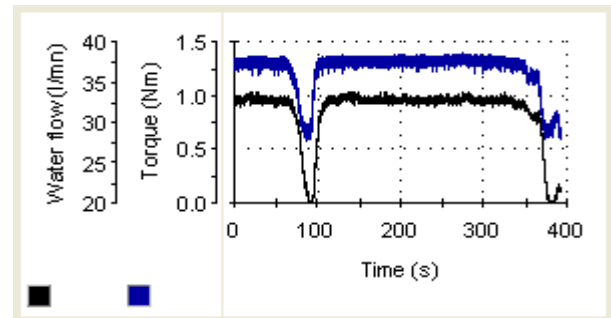


FIG.20. EVOLUTION OF ELECTROMAGNETIC TORQUE AND FLOW RATE

B. IC results

To test the incremental conductance approach, an actual randomly scenario of insolation has been captured, as shown in Fig.21, and the evolution of some physical variables are recorded. Fig.22 gives the evolution of the extracted power P_{pv} , the estimated maximum power P_{pv_opt} .

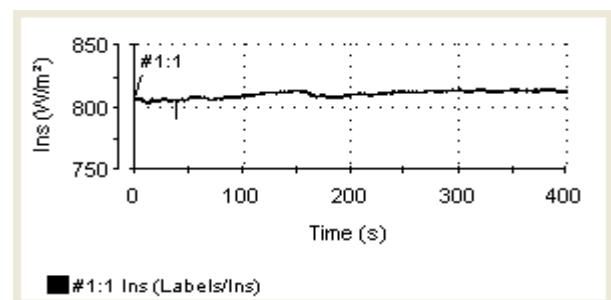


FIG.21. EVOLUTION OF INSOLATION

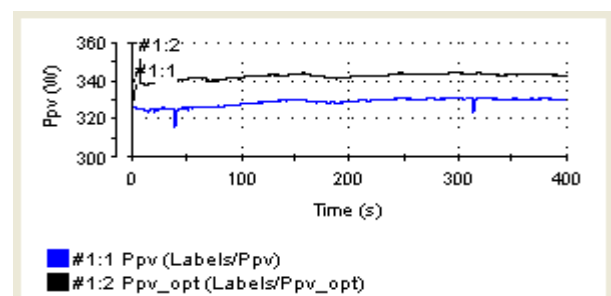


FIG.22. EXTRACTED, OPTIMAL AND EFFICIENCY

The maximum efficiency is more than 96% as shown in Fig.23. Finally, the operating point displacement for the

proposed scenario is given in Fig.24. Fig.25 shows that the PVG voltage is varied between 145V and 150V. These results show clearly the effectiveness of this control approach.

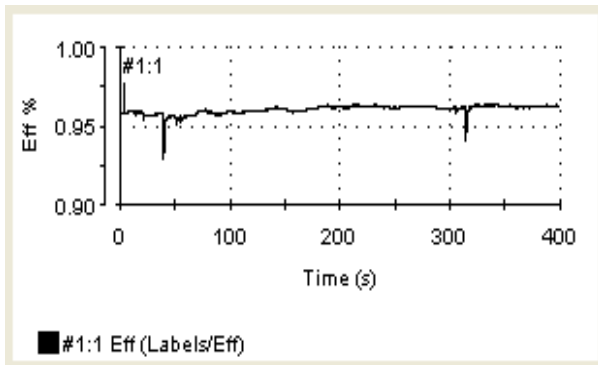


FIG.23. EVOLUTION OF EFFICIENCY

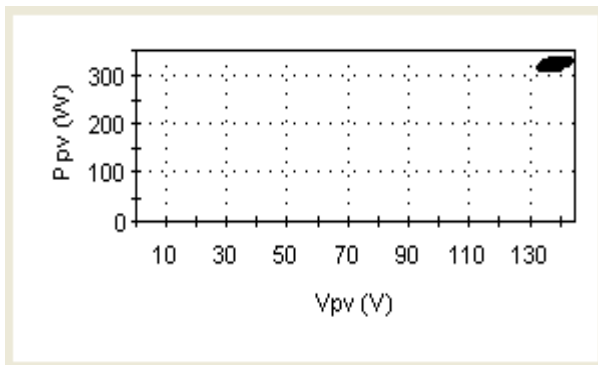


FIG.24. MPP EVOLUTION

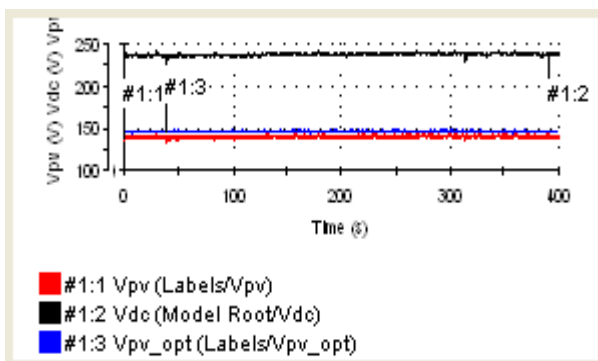


FIG.25. EVOLUTION OF V_{dc} , V_{pv} AND V_{pv_opt}

The same for this control the ratio between V_s and ω_s is constant for a nominal flux, Fig.26. Fig.27 shows that the flow rate and the torque move in the same direction as the insolation.

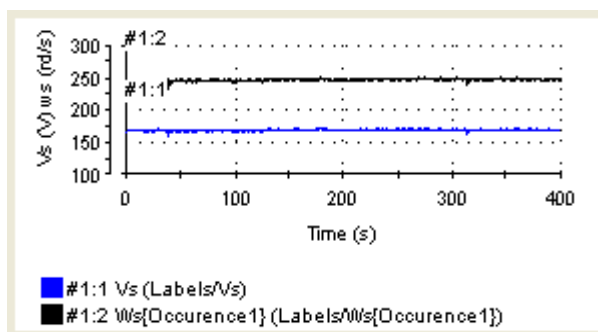


FIG.26. EVOLUTION OF STATOR VOLTAGE AND PULSATION

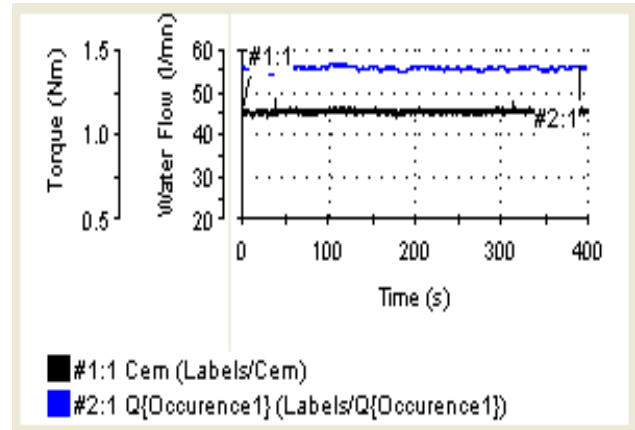


FIG.27. EVOLUTION OF ELECTROMAGNETIC TORQUE AND FLOW RATE

V. DISCUSSION AND COMPARATIVE STUDY

The MPPT techniques are simple algorithms that do not require analog circuit to realize some functions as comparator, additional circuit...

The CV approach kept constant the real voltage generated by PVG around a reference value chosen by an experimental test. For a random scenario of insolation, the efficiency is related to the choice of the reference voltage. This approach is simple and inexpensive.

The MPPT technique incremental conductance does not require knowledge of the GPV parameters and it is easy to implement. We note here that the voltage generated by PVG varies around the voltage that corresponds to operation at maximum power, confirming the validity of the approach. The advantage of this algorithm doesn't require a database.

VI. CONCLUSION

The implementation in real-time of a test bench based on a STM32F4 microcontroller of the entire chain water pumping system is controlled by two maximum power extraction approaches CV and IC. The first is not sensitive to parametric variations, here; the operating point is around the point at maximum power. So, the efficiency depends on the choice of the reference voltage.

The IC method finds directly the maximum power point. We also noticed that we got a very good efficiency for this approach. For the used scenario of insolation, the efficiency can reach 97% for IC approach. In this work the usefulness of these MPPT approaches developed to solve the problem of degradation of PVG performance following the change of insolation is developed. The MPPT control could significantly increase the efficiency of energy production from the PVG and as consequence the performance of the PV water pumping system. The experiment results prove positively that constant voltage control and the IC MPPTs can reach the intended MPP. The cost of the realized MPPT controller is acceptable.

APPENDIX.1. THE ELECTRICAL SPECIFICATIONS OF THE SOLAR MODULE

| | |
|-------------------------|--------------------|
| Name Manufacturer | TITAN |
| Description | STP-50-01 |
| Cell types | Polycrystalline |
| Cell size | 100cm ² |
| Cell number | 36 |
| Rated power | 50Wc |
| Power tolerance | ± 5% |
| Optimal voltage | 17.2V |
| Optimal current | 2.9A |
| Open circuit voltage | 21V |
| Short circuit current | 3.4A |
| Efficiency | 11.3% |
| Manufacturer's warranty | 20 years |

APPENDIX.2. INDUCTION MACHINE CHARACTERISTICS

| | |
|-------------------|--------------------------|
| Rated power | $P_n = 0.61\text{kW}$ |
| Stator resistance | $R_s = 17.68\Omega$ |
| Rotor resistance | $R_r = 19.1\Omega$ |
| Stator inductance | $L_s = 0.6877\text{H}$ |
| Rotor inductance | $L_r = 0.6811\text{H}$ |
| Mutual inductance | $M = 0.6561\text{H}$ |
| Moment of inertia | $J = 0.0001\text{kgm}^2$ |
| Rated torque | $T_n = 1.9\text{Nm}$ |
| Rated Voltage | $V_n = 220\text{V}$ |
| Rated current | $I_n = 1.45\text{A}$ |
| Number of poles | $p = 1$ |

REFERENCES

- [1] A. Saadi , A. Moussi. (2006). Optimisation of Chopping ratio of Back-Boost Converter by MPPT technique with a variable reference voltage applied to the Photovoltaic Water Pumping System. IEEE ISIE 2006, Montreal, Quebec, Canada.
- [2] A. Durgadevi, S. Arulselvi, S.P.Natarajan. (2.11). Study and Implementation of Maximum Power Point Tracking (MPPT) Algorithm for Photovoltaic Systems. 978-1-61284-379-7/11\$26.00_c IEEE.
- [3] Guan-Chyun Hsieh, Hung-I Hsieh, Cheng-Yuan Tsai, Chi-Hao Wang. (2013). Photovoltaic Power Increment-Aided Incremental-Conductance MPPT With Two-Phased Tracking. IEEE TRANSACTIONS ON POWER ELECTRONICS, VOL. 28, NO. 6.
- [4] Mohammad A. S. Masoum, Hooman Dehbonei, Ewald F. Fuchs. (2002). Theoretical and Experimental Analyses of Photovoltaic Systems With Voltage- and Current-Based Maximum Power-Point Tracking. IEEE TRANSACTIONS ON ENERGY CONVERSION, VOL. 17, NO. 4.
- [5] Yousif I. Al Mashhadany. (2012). Design and Implementation of Electronic Control Trainer with PIC Microcontroller. Intelligent Control and Automation, 2012, 3, 222-228.
- [6] Issam Houssamo, Fabrice Locment, Manuela Sechilariu. (2010). Maximum power tracking for photovoltaic power system: Development and experimental comparison of two algorithms, Renewable Energy 35 (2010) 2381e2387.
- [7] R. Akkaya , A.A. Kulaksız, O . Aydog˘du. (2007). DSP implementation of a PV system with GA-MLP-NN based MPPT controller supplying BLDC motor drive. Energy Conversion and Management 48(2007) 210-218.
- [8] S. Jiang, D. Cao, Y. Li, and F. Z. Peng. (2012). Grid-connected boost-half-bridge photovoltaic microinverter system using repetitive current control and maximum power point tracking. IEEE Trans. Power Electron., vol. 27, no. 11, pp. 4711–4722.
- [9] Mohammad A.S. Masoum, Hooman Dehbonei, Ewald F. Fuchs. (2002). Theoretical and Experimental Analyses of Photovoltaic Systems With

- Voltage-and Current-Based Maximum Power-Point Tracking. IEEE Transactons of Energy Conversin, Vol. 17, No.4.
- [10] NajetRebei, Ali Hmidet, Rabiaa Gammoudi,Othman Hasnaoui. (2015). Implementation of photovoltaic water pumping system withMPPT controls. Higher Education Press and Springer-Verlag Berlin Heidelberg .
- [11] Rabiaa Gammoudi, NajetRebei, Othman Hasnaoui. (2014). Implementation MPPT approaches of PV system. International Journal of Renewable Energy, Vol. 9, No. 2.
- [12] A. Mellit, H. Mekki , A. Messai , H. Salhi. (2010). FPGA-based implementation of an intelligent simulator for stand-alone photovoltaic system. Expert Systems with Applications 37 (2010) 6036–605.
- [13] A. Safari and S. Mekhilef. (2011). Simulation and hardware implementation of incremental conductance MPPT with direct control method using Cukconverter. IEEE Trans. Ind. Electron., vol. 58, no. 4, pp. 1154–1161.
- [14] Ali Hmidet, Najet Rebei, Othman Hasnaoui. (2015). Experimental studies and performance Evaluation of MPPT Control Strategies for Solar-Powered Water Pumps. Tenth Interntional Conference on Ecological Vehicles and Renewable Energies (EVER).